

# Forecasting Andean rainfall and crop yield from the influence of El Niño on Pleiades visibility

Benjamin S. Orlove\*†, John C. H. Chiang† & Mark A. Cane†

\* Department of Environmental Science and Policy, University of California, Davis, California 95616, USA

† Lamont-Doherty Earth Observatory of Columbia University, Palisades, New York 10964, USA

Farmers in drought-prone regions of Andean South America have historically made observations of changes in the apparent brightness of stars in the Pleiades around the time of the southern winter solstice in order to forecast interannual variations in summer rainfall and in autumn harvests. They moderate the effect of reduced rainfall by adjusting the planting dates of potatoes, their most important crop<sup>1</sup>. Here we use data on cloud cover and water vapour from satellite imagery, agronomic data from the Andean altiplano and an index of El Niño variability to analyse this forecasting method. We find that poor visibility of the Pleiades in June—caused by an increase in subvisual high cirrus clouds—is indicative of an El Niño year, which is usually linked to reduced rainfall during the growing season several months later. Our results suggest that this centuries-old method<sup>2</sup> of seasonal rainfall forecasting may be based on a simple indicator of El Niño variability.

We reviewed anthropological accounts of indigenous Aymara- and Quechua-speaking farmers of the Peruvian and Bolivian Andes (hereafter central Andes). In 12 villages<sup>3–16</sup> (see Fig. 1a, Table 1), the inhabitants observe the Pleiades in late June in order to forecast the weather during the growing season (October–May). Observations often begin around 15 June and culminate on 24 June, the festival of San Juan. They occur an hour or two before dawn, when the Pleiades are located low over the horizon to the northeast.

Four different attributes of the Pleiades were reported (Table 1). Two attributes are directly related to the relative clarity or transparency of the sky: the brightness of the cluster and the timing of the heliacal rise (the date of the first appearance in the eastern pre-dawn sky). The third attribute, the apparent size of the Pleiades, may also be related to atmospheric clarity. On nights when the dimmest stars are visible, the Pleiades will appear to be 25% larger in diameter than on less clear nights (Fig. 2). The fourth attribute, the relative position of the brightest star in the Pleiades, is reported in various ways in different villages. Our interpretation of this attribute is

uncertain, but the brightest star in the cluster may appear to shift its position when the dimmest stars are no longer visible.

The villagers use these attributes to forecast the timing and quantity of rains and to estimate the size of the harvest, concentrated between March and May of the following year. The attributes associated with clearer skies indicate earlier and more abundant rains and larger harvests, while the opposite is linked to less clear skies. If poor rains are predicted, villagers postpone the planting of potatoes. A shallow-rooted crop, potatoes are most vulnerable to drought at planting, when low soil moisture inhibits root formation<sup>17</sup>, and again a few weeks later when the sprouts have depleted the residual moisture in the seed tubers. Lack of soil moisture at that time reduces the number of stems per plant and the overall yield<sup>18</sup>. By delaying for 4–6 weeks after the usual October–November planting time, the farmers reduce these risks by starting the potato crop in months of higher rainfall.

This forecasting system is likely to be more than four centuries old. The Incas, who unified the central Andes in the fifteenth century and were in turn conquered by the Spaniards in 1532, worshipped and closely observed the Pleiades<sup>19</sup>. It is not established that they used its appearance to forecast weather, but several sources do document such forecasts soon after the conquest. In the late sixteenth century, some central Andean villages celebrated the Pleiades in June<sup>20</sup>, some noted the date of its heliacal rise<sup>21</sup>, and some made forecasts that linked a large apparent size of the Pleiades with good harvests and a small size with poor harvests<sup>2</sup>. The general importance of the Pleiades in Andean astronomy is suggested by its prominent position in a seventeenth-century cosmological chart<sup>22</sup> (see Supplementary Information).

We now examine whether the visibility of the Pleiades from the central Andes in June is correlated with harvests in the following year. We use high cloud as a measure of atmospheric transparency (see below). The International Satellite Cloud Climatology Project (ISCCP) nadir-viewing satellite cloud data set provides data on high cloud cover over the central Andes<sup>23</sup>. For a measure of harvests, we use yield for Puno department, located near the centre of the region in which forecasts are made. Figure 1a shows, as contours, the rank correlation between high cloud and potato harvest, indicative of the degree of correspondence between these two variables. Because of the low angle of the Pleiades at the time of observation, the relevant region is about 175 km to the northeast of the villages, where correlations are in the –0.5 to –0.6 range. In the five cases for which independent data on forecast and outcome are available, the forecasts have been accurate (see Supplementary Information).

To account for this correlation, we examine the links of high cloud amount and potato harvest, as well as precipitation, to El Niño/Southern Oscillation (ENSO). ENSO is an interannual climate fluctuation originating from large-scale dynamical interactions

Table 1 Village data on Pleiades observations

| Village       | Department | Country | Latitude (°S) | Longitude (°W) | Elevation (m) | Date                   |                     |               | Attribute of Pleiades |                          |      | Modification of Planting dates? | Ref.          |                            |
|---------------|------------|---------|---------------|----------------|---------------|------------------------|---------------------|---------------|-----------------------|--------------------------|------|---------------------------------|---------------|----------------------------|
|               |            |         |               |                |               | Early June observation | 24 June observation | After 24 June | Brightness            | Date of first appearance | Size |                                 |               | Position of brightest star |
| Concepción    | Junín      | Peru    | 11.9          | 75.2           | 3,300         | Not mentioned          | Yes                 | No            | No                    | Not mentioned            | No   | Yes                             | Yes           | 3                          |
| Misminay      | Cusco      | Peru    | 13.0          | 72.0           | 3,400         | No                     | Yes                 | No            | Yes                   | No                       | Yes  | Yes                             | Yes           | 4                          |
| Quispillacta  | Ayacucho   | Peru    | 13.6          | 74.4           | 3,300         | No                     | Yes                 | No            | Yes                   | No                       | Yes  | Yes                             | Yes           | 5                          |
| Kauri         | Cusco      | Peru    | 13.6          | 71.5           | 4,300         | No                     | Yes                 | Yes           | No                    | No                       | No   | Yes                             | Yes           | 6                          |
| Sallaq        | Cusco      | Peru    | 13.7          | 71.6           | 3,200         | Not mentioned          | Yes                 | No            | No                    | Not mentioned            | No   | Yes                             | Yes           | 7                          |
| Sicuaní       | Cusco      | Peru    | 14.3          | 71.2           | 3,550         | Not mentioned          | Yes                 | No            | Yes                   | Not mentioned            | Yes  | No                              | Not mentioned | 5, 8                       |
| Maranganí     | Cusco      | Peru    | 14.4          | 71.1           | 3,600         | No                     | No                  | Yes           | Yes                   | No                       | Yes  | No                              | Not mentioned | 9                          |
| Cuyo Cuyo     | Puno       | Peru    | 14.5          | 69.5           | 3,750         | Yes                    | Yes                 | No            | Yes                   | Yes                      | No   | No                              | Yes           | 10, 11                     |
| Qorpa         | La Paz     | Bolivia | 16.5          | 68.7           | 3,850         | Yes                    | Yes                 | No            | Yes                   | Yes                      | No   | Yes                             | Yes           | 12                         |
| Irpa Chico    | La Paz     | Bolivia | 16.7          | 68.4           | 3,800         | Yes                    | No                  | No            | No                    | Yes                      | No   | No                              | Yes           | 13, 14                     |
| Chambi Grande | La Paz     | Bolivia | 17.6          | 68.4           | 3,700         | Not mentioned          | Yes                 | No            | Yes                   | Not mentioned            | Yes  | No                              | Yes           | 15                         |
| Chayantaka    | Potosí     | Bolivia | 18.5          | 66.5           | 3,800         | Yes                    | Yes                 | No            | Yes                   | Yes                      | Yes  | No                              | Yes           | 16                         |

Data collected from the 12 villages, as reported in the anthropological accounts of farmers in the Peruvian and Bolivian Andes<sup>3–16</sup>. The villages are listed in the order that corresponds to their numbering in Fig. 1a. Ten of the 12 villages have a Pleiades observation on 24 June. The most common attribute of the Pleiades reported is the brightness (8 villages). The size of the cluster and the position of the brightest star are observed in half of the villages (6 villages each), and is the date of first appearance (4 of the 8 villages for which data are reported). A large majority (at least 10) of the villages modifies their planting dates in response to the forecast.

between the ocean and atmosphere of the tropical Pacific, and has the largest effect on short-term global climate variability of any such fluctuation. ENSO influences a number of atmospheric variables in the central Andes. Atmospheric extinction data measured by the Stratospheric Aerosol and Gas Experiment II (SAGE II) solar occultation instrument show that tropic cirrus cloud cover increases in warm ENSO years relative to cold ENSO years over the central Andes<sup>24</sup>. At the representative altitude of 14.5 km, the cloud amount increased from around 35% in cold ENSO years to 50% in warm ENSO years. Though too much high cloud could totally mask out the Pleiades, the SAGE II data show that most tropical high cloud is subvisual (with optical thickness <0.03) from just over 50% of cloud amount at the 10.5-km level to almost 100% above 16 km. We estimate the average optical thickness of the 10–19 km cloud layer to be between 0.05 and 0.35, with the major uncertainty due to uncertainty in the extinction coefficients of the optically thicker clouds in this layer. Change in cloud amount between cold and warm ENSO years thus leads to an estimated optical thickness change between 0.01 and 0.1, yielding a change in Pleiades brightness of around 0.1 to 1 magnitude. This shift is sufficient to visibly reduce the apparent brightness of the Pleiades between cold and warm years.

Increase in cloud frequency in the SAGE II data set is corroborated by high-cloud data from the ISCCP dataset<sup>23</sup> (Fig. 1b). Optically thin (<0.1 at 0.6 μm) clouds are at the detection limit

for the ISCCP<sup>25</sup>, but even if the optically thin clouds are not detected, the high-cloud correlation with ENSO implies more moist conditions during warm years and an increased likelihood of thin clouds.

We considered other factors that might influence atmospheric visibility in the central Andes in June. Using a reanalysis data set<sup>26</sup>, we found that upper-level winds increase in warm ENSO years. Though the accompanying decrease in vertical stability might lead to more turbulence, this change would have little direct effect on visibility. ENSO is also significantly correlated with total column-integrated precipitable water northeast of the villages, as estimated by mean monthly data from the Total Ozone Vertical Sounder (TOVS)<sup>23</sup>. The increase in total precipitable water from cold to warm ENSO years is around 10–20% of the mean amount, and may contribute to the formation of thin high cloud. The reanalysis data set<sup>26</sup> indicates that the surface relative humidity of about 60–70% increases by about 5–10% in warm years. Standard formulas<sup>27</sup> indicate that this increase would alter apparent magnitude by about 0.1, a level too small to be appreciated by the naked-eye observer. We conclude that the significant changes in visibility are attributable to changes in high cloud alone. However, our confidence in the link between ENSO and shifts in cloud cover is bolstered by the consistent relationship found within independent data sets between ENSO and other atmospheric variables.

We note that synoptic variability in atmospheric conditions

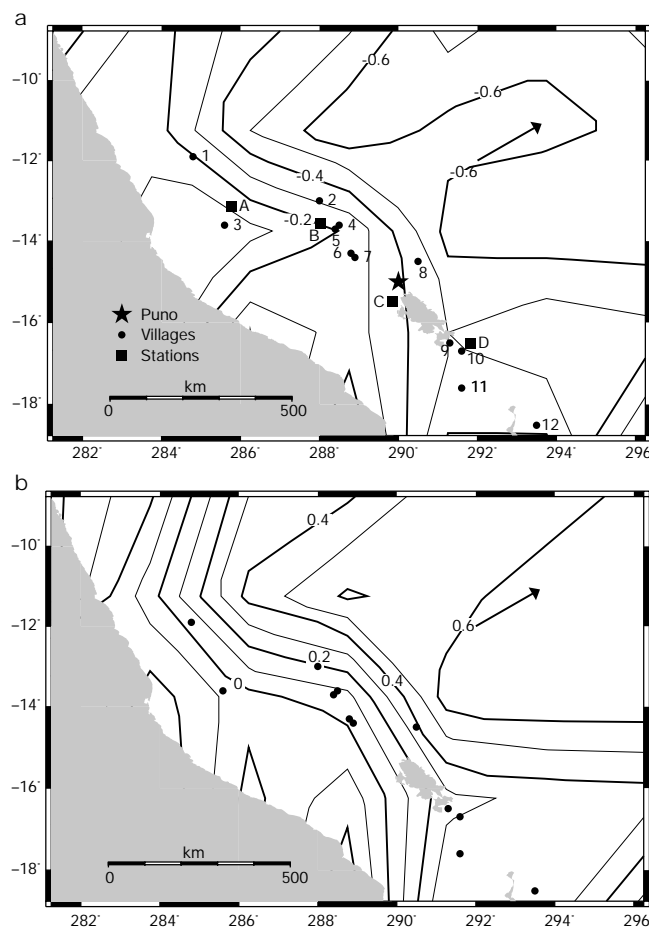


**Figure 1** Correlations with central Andean high cloud in late June. Contours show rank correlations with the ISCCP C29 GMT anomalous high-cloud amount over late June (see text). Filled circles indicate location of the 12 villages listed in Table 1, filled squares the location of the four meteorological stations, and the star the approximate geographical centre of Puno department. The arrow indicates the azimuth of Pleiades observations during late June. Late June anomalous high cloud is computed by linearly interpolating the June and July anomalous monthly cloud data to 24 June, assuming that monthly

mean data are centred on the 15th of the month. The exceptions are 1983, where we take July anomalies only, and 1991, where we take June anomalies only (ISCCP data runs from July 1983 to June 1991). **a**, Rank correlation with potato yield in Puno department in the year following the June cloud data. Annual potato yield is computed from August to the following July. **b**, Rank correlation with the NINO3 index (the sea surface temperature anomaly averaged over 5° S–5° N, and 150° W–90° W) averaged over November to January (NINO3NDJ) following June cloud data.

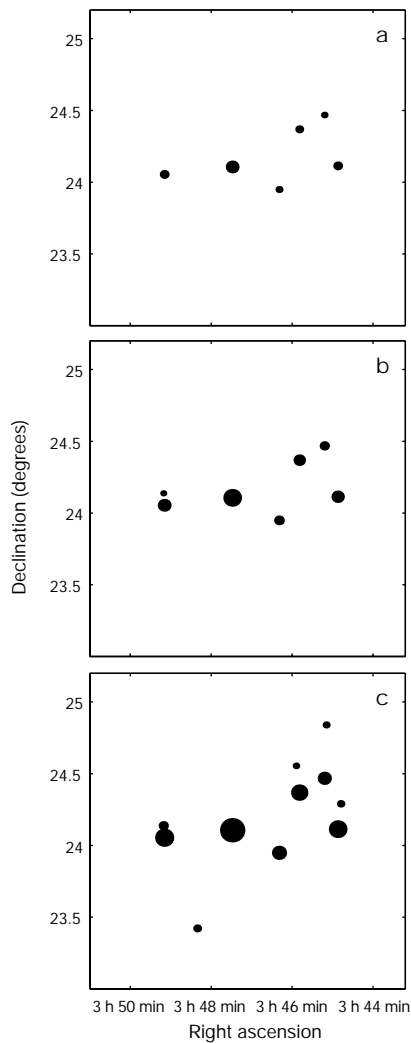


**Figure 2** A diagram of the stars in the Pleiades of visual magnitude 6.0 or brighter. Although human visual acuity is often reduced at high elevations above sea level, suggesting that a lower threshold would be appropriate in this case, we note that hypoxia, the cause of this diminution, is not a problem for the populations under study<sup>30</sup>. In this diagram, the size of each star is proportional to its intensity. We show three frames representing the Pleiades in steps of a 0.75 change in apparent magnitude, to show the effect of different observing conditions. The stars can be grouped into three brightness classes. The brightest group consists of only one star (Alcyone or 25 Tauri) of magnitude 2.90. There is a gap of 0.72 magnitude between this star and the intermediate group, of magnitude 3.62–4.30. A gap of 0.79 magnitude separates this group from the dimmest group, of magnitude 5.09–5.80. The axis of the six brightest stars in the Pleiades has an apparent breadth of 59 arcmin. For comparison, the moon’s apparent diameter is less than 32 arcmin.

implies that a single viewing on 24 June at the festival of San Juan could be misleading. It is a common but not universal practice (Table 1) to make observations over a number of days, increasing the likelihood of registering the ENSO signal correctly. Additional research with a larger sample of villages would be needed to ascertain the range of observing practices. Are they near ‘optimal’ for the purpose of prediction, or are they strongly shaped by social and cultural factors?

That drought conditions in the central Andes are associated with El Niño has been documented<sup>28,29</sup>. To further analyse this relation, we examined precipitation data between July 1962 and June 1988 from the 4 stations with nearly complete records representative of the region occupied by the 12 villages: Ayacucho, Cusco and Juliaca in Peru, and La Paz in Bolivia (Fig. 1a). After removing the

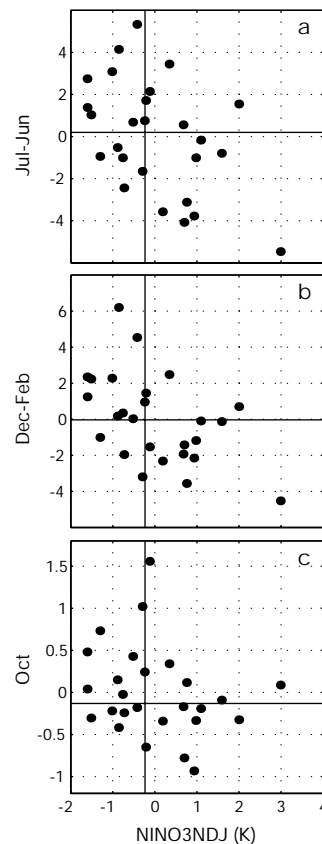


**Figure 3** Central Andean rainfall anomalies and El Niño. Shown are scatterplots of a central Andes precipitation anomalies index versus the NINO3NDJ index; the latter is the NINO3 index averaged over November–January. All timeseries were detrended. The precipitation index in **a** has been summed over the entire year from July to the following June; in **b**, summed over the high-rainfall months of December–February; and in **c**, measured for October, the onset of the rainy season. The solid lines, at the value of the median for each axis, divide the data into high and low categories. All cases suggest that lower rainfall is associated with El Niño events. Station precipitation data are from the NOAA Baseline Climatological Dataset, compiled by the National Climatic Data Center (Asheville, North Carolina, USA) and the Environmental Research Laboratory (Boulder, Colorado, USA).

climatological monthly mean at each station, we normalized each time series by its standard deviation. We then averaged the four normalized anomaly time series to create an index of central Andes precipitation anomalies. When data were missing (about 9% of the time), we estimated the index as the average of the remaining available station values. Other indices (total rainfall; the first principal component) gave quite similar results.

Figure 3a shows that precipitation anomalies summed over the entire year (July to the following June) are likely to be lower during warmer El Niño years. Precipitation anomalies summed over the highest-precipitation months of December to February show an even tighter relationship (Fig. 3b). October precipitation is also suppressed during El Niño years, suggesting a later onset of the rainy season (Fig. 3c). In keeping with the type of forecasts made by the Andeans, we also divide (‘bin’) the data into high/low precipitation, and high/low NINO3, and apply  $\chi^2$  tests to measure the significance of the relations. (NINO3 is the sea surface temperature anomaly, averaged over 5° S–5° N and 150° W–90° W.) Our ability to test the significance of these relationships is limited by the relatively small amount of data; nevertheless, the test shows high significance (exceeding the 95% level) for the December–February precipitation relationship. The other two relationships shown in Fig. 3 are less significant (around the 75% level).

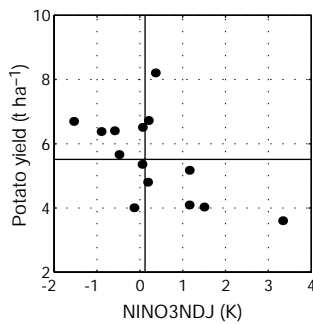


**Figure 4** Central Andean harvests and El Niño. Shown are potato yields (in tonnes per hectare) for Puno department plotted against NINO3NDJ, 1980–81 to 1993–94. The solid lines represent median values for each axis.

Given the sensitivity of potatoes to drought, this reduction in precipitation may account for part of the relationship between June high-cloud amount and potato harvests (Fig. 1a). A more complete analysis of the effect of climate on crops must include other climatic variables, most notably temperature. In fact, we find a strong monotonic relationship between ENSO and mean monthly temperatures in the central Andes region, with warmer mean temperatures in the central Andes during El Niño years. Though the effect of temperature on crop growth is not obvious, the consequence of ENSO for potato yields is convincingly demonstrated from preliminary analysis of potato-yield data from Puno department near Lake Titicaca (Fig. 4). Significant reductions in potato yield are observed for warm ENSO years. A 2-bin  $\chi^2$  test shows significance at the 90% level. The linear correlation value is  $-0.6$ . □

Received 22 March; accepted 11 November 1999.

1. Zimmerer, K. S. *Changing Fortunes: Biodiversity and Peasant Livelihood in the Peruvian Andes* (Univ. California Press, Berkeley, 1996).
2. Salomon, F. & Urioste, G. L. *The Huarochiri Manuscript: A Testament of Ancient and Colonial Andean Religion* (Univ. Texas Press, Austin, 1991 [c. 1608]).
3. Ballón Aguirre, E., Cerrón Palomino, R. O. & Chambí Apaza, E. *Vocabulario Razonado de la Actividad Agraria Andina. Terminología Agraria Quechua*. (Centro de Estudios Regionales Andinos "Bartolomé de Las Casas", Cusco, 1992).
4. Urton, G. *At the Crossroads of the Earth and The Sky: An Andean Cosmology* (Univ. Texas Press, Austin, 1981).
5. Grillo Fernández, E., Quiso Choque, V., Rengifo Vásquez, G. & Valladolid Rivera, J. *Crianza Andina de la Chacra* (Proyecto Andino de Tecnología Campesina, Lima, 1994).
6. Mishkin, B. Cosmological ideas among the Indians of the southern Andes. *J. Am. Folklore* 53, 225–241 (1940).
7. Morote Best, E. La fiesta de San Juan, el Bautista. *Arch. Peruanos Folklore* 1, 160–200 (1953).
8. Orlove, B. S. Two rituals and three hypotheses: an examination of solstice divination in southern highland Peru. *Anthropol. Quart.* 52, 86–98 (1979).
9. Lira, J. A. *Farmacopea Tradicional Indígena y Prácticas Rituales* (El Condor, Lima, 1946).
10. Camino, A., Recharte, J. & Bidegaray, P. *La Tecnología en el Mundo Andino. Runakunap Kawsaynikupaq Rurasankunapaq* Vol. 1 (eds Lechtman, H. & Soldi, A. M.) 261–281 (Universidad Nacional Autónoma de México, Mexico City, 1981).
11. Goland, C. *Cultivating Diversity: Field Scattering as Agricultural Risk Management in Cuyo Cuyo, Dept. of Puno, Peru* (Working Paper No. 4, Research Project on Production, Storage and Exchange in a Terraced Environment on the Eastern Andean Escarpment, Department of Anthropology, Univ. North Carolina, Chapel Hill, 1992).
12. Kolata, A. *Valley of the Spirits: A Journey into the Lost Realm of the Aymara* (Wiley, New York, 1996).
13. Carter, W. E. & Mamani, M. *Irpa Chico: Individuo y Comunidad en la Cultura Aymara* (Juventud, La Paz, 1982).
14. Mamani, M. in *Raíces de América: el Mundo Aymara* (ed. Albó, X.) 75–131 (Alianza, Madrid, 1988).
15. Yampara Huarachi, S. in *La Cosmovisión Aymara* (eds van den Berg, H. & Schiffers, N.) 143–186 (UCB/HISBOL, La Paz, 1992).
16. Kraft, K. E. *Andean Fields and Fallow Pastures: Communal Land Use Management under Pressures for Intensification*. Thesis, Univ. Florida (1995).
17. Beukema, H. P. & van de Zaag, D. E. *Introduction to Potato Production* (Pudoc, Wageningen, 1990).
18. MacKerron, D. K. L. & Jeffries, R. A. The distribution of tuber sizes in droughted and irrigated crops of potato. I. Observations on the effect of water stress on graded yields from differing cultivars. *Potato Res.* 31, 269–278 (1988).
19. Bauer, B. S. & Dearborn, D. S. P. *Astronomy and Empire in the Ancient Andes: The Cultural Origins of Inca Sky Watching*. (Univ. Texas Press, Austin, 1995).
20. de Arriaga, P. J. *The Extirpation of Idolatry in Peru* (Univ. Kentucky Press, Lexington, 1968 [1621]).
21. Anonymous Jesuit priest Misión de las provincias de los Huachos y Yauyos. *Rev. Histórica* (Lima) 6, 180–197 (1919).
22. de Santillán, F., Valera, B. & Pachacuti, J. de S. C. *Tres Relaciones de Antigüedades Peruanas* (Guaranía, Asunción, 1950).

23. Rossow, W. B. & Schiffer, R. A. ISCCP cloud data products. *Bull. Am. Meteorol. Soc.* 72, 2–20 (1991).
24. Kent, G. S. *et al.* Surface temperature related variations in tropical cirrus cloud as measured by SAGE II. *J. Clim.* 8, 2577–2594 (1995).
25. Liao, X., Rossow, W. B. & Rind, D. Comparison between SAGE II and ISCCP high-level clouds 1. Global and zonal mean cloud amounts. *J. Geophys. Res.* 100, 1121–1135 (1995).
26. Kalnay, E. *et al.* The NCEP/NCAR 40 year reanalysis project. *Bull. Am. Meteorol. Soc.* 77, 437–471 (1996).
27. Schaefer, B. E. Astronomy and the limits of vision. *Vistas Astron.* 36, 311–361 (1993).
28. Thompson, L. G., Mosley-Thompson, E. & Arnao, B. J. El Niño–Southern Oscillation events recorded in the stratigraphy of the tropical Quelccaya ice cap, Peru. *Science* 226, 50–53 (1984).
29. Aceituno, P. On the functioning of the Southern Oscillation in the South American sector. Part I: Surface climate. *Mon. Weath. Rev.* 116, 505–524 (1988).
30. Frisancho, A. R. *et al.* Developmental, genetic and environmental components of aerobic capacity at high altitude. *Am. J. Phys. Anthropol.* 96, 431–442 (1995).

Supplementary information is available on Nature's World-Wide Web site (<http://www.nature.com>) or as paper copy from the London editorial office of Nature.

**Acknowledgements**

We thank G. Urton for insights into Andean ethnoastronomy, G. Rasmussen for discussions on visibility and cirrus cloud, G. Scott for providing potato yield data for Puno department, Peru, and R. Bishop, K. Cook, D. Dearborn, D. Helfand, A. Kaplan, G. Kiladis, J. Lenters, M. Sarazin and B. Schafer for comments. M.A.C. thanks B. D'Achille for first making him aware of the Andean forecasting scheme.

Correspondence and requests for materials should be addressed to B.S.O. (e-mail: bsorlove@ucdavis.edu).

**Channelized fluid flow in oceanic crust reconciles heat-flow and permeability data**

A. T. Fisher\* & K. Becker†

\* Earth Sciences Department, University of California, Santa Cruz, California 95064, USA

† Division of Marine Geology and Geophysics, Rosenstiel School of Marine and Atmospheric Sciences, University of Miami, Miami, Florida 33145, USA

Hydrothermal fluid circulation within the sea floor profoundly influences the physical, chemical and biological state of the crust and the oceans. Circulation within ridge flanks (in crust more than 1 Myr old) results in greater heat loss<sup>1–3</sup> and fluid flux<sup>4</sup> than that at ridge crests and persists for millions of years, thereby altering the composition of the crust and overlying ocean<sup>5,6</sup>. Fluid flow in oceanic crust is, however, limited by the extent and nature of the rock's permeability<sup>7</sup>. Here we demonstrate that the global data set of borehole permeability measurements in uppermost oceanic crust<sup>7–9</sup> defines a trend with age that is consistent with changes in seismic velocity<sup>10,11</sup>. This trend—which indicates that fluid flow should be greatly reduced in crust older than a few million years—would appear to be inconsistent with heat-flow observations, which on average indicate significant advective heat loss in crust up to 65 Myr old<sup>3</sup>. But our calculations, based on a lateral flow model, suggest that regional-scale permeabilities are much higher than have been measured in boreholes. These results can be reconciled if most of the fluid flow in the upper crust is channelized through a small volume of rock, influencing the geometry of convection and the nature of fluid–rock interaction.

Permeabilities have been measured in oceanic crustal boreholes using a drill-string packer, a device that hydraulically seals a borehole so that fluid can be pumped into the formation and transient changes in pressure can be monitored<sup>7</sup>. These measurements yield “bulk” permeabilities close to the borehole, assumed to be distributed evenly within the isolated interval. Other methods, including interpretation of temperature logs within upper basement<sup>12,13</sup>, and modelling of subsurface tidal response recorded by pressures in